land

MDPI

Review

Spatial–Temporal Variations in Soil Organic Carbon and Driving Factors in Guangdong, China (2009–2023)

Mi Tian [1,2], Chao Wu [1,2,*], Xin Zhu [3], Qinghai Hu [1,2,*], Xueqiu Wang [1,2], Binbin Sun [1,2], Jian Zhou [1,2], Wei Wang [1,2], Qinghua Chi [1,2], Hanliang Liu [1,2], Yuheng Liu [1,2], Jiwu Yang [3] and Xurong Li [3]

[1] Key Laboratory of Geochemical Exploration, Institute of Geophysical and Geochemical Exploration, Langfang 065000, China; tianmi62080608@126.com (M.T.); wxueqiu@mail.cgs.gov.cn (X.W.); sbinbin@mail.cgs.gov.cn (B.S.); zhoujian@mail.cgs.gov.cn (J.Z.); wangwei@mail.cgs.gov.cn (W.W.); cqinghua@mail.cgs.gov.cn (Q.C.); lhanliang@mail.cgs.gov.cn (H.L.); liuyuheng@mail.cgs.gov.cn (Y.L.)
[2] International Centre on Global-Scale Geochemistry, Langfang 065000, China
[3] Guangdong Geological Survey Institute, Guangzhou 510440, China; zhuxin@gdgsi.com (X.Z.); yangjiwu@gdgsi.com (J.Y.); lixurong@gdgsi.com (X.L.)
* Correspondence: wuchao@mail.cgs.gov.cn (C.W.); huqinghai@mail.cgs.gov.cn (Q.H.)

Abstract: Spatial–temporal variation in soil organic carbon is an important factor for national targets to mitigate climate change and land degradation impacts. In this research, we took Guangdong Province of China as the study area, evaluated the spatial–temporal distributions of soil organic carbon using data from three China Geochemical Baseline projects (conducted in 2009, 2016, and 2023, respectively), and quantified the main driving factors of spatial–temporal variations in soil organic carbon using the random forest algorithm, further predicting the density and inventories of soil organic carbon. The results demonstrate that the mean value of SOC in Guangdong in 2009 was 0.81%; in 2016 it was 1.13%; and in 2023 it was 1.02%. The inventories of soil organic carbon (0–30 cm) in Guangdong Province were 0.61 Pg in 2009, 0.74 Pg in 2016, and 0.62 Pg in 2023. Soil in Guangdong acted as a carbon sink from 2009 to 2023 as a whole, and the most important driving force behind spatial–temporal variations in soil organic carbon was temperature, followed by precipitation and vegetation cover.

Keywords: soil organic carbon; spatial–temporal variations; random forest; inventories

Citation: Tian, M.; Wu, C.; Zhu, X.; Hu, Q.; Wang, X.; Sun, B.; Zhou, J.; Wang, W.; Chi, Q.; Liu, H.; et al. Spatial–Temporal Variations in Soil Organic Carbon and Driving Factors in Guangdong, China (2009–2023). *Land* **2024**, *13*, 1096. https://doi.org/10.3390/land13071096

Academic Editor: Nick B. Comerford

Received: 20 June 2024
Revised: 15 July 2024
Accepted: 17 July 2024
Published: 20 July 2024

1. Introduction

Spatial–temporal variations in soil organic carbon (SOC) are one of the vital factors affecting global carbon cycles, as well as global climate change [1]. The Third Assessment Report of IPCC pointed out that, since the 1760s, global temperature has shown a significant warming phenomenon, due to rapidly increasing CO_2 in the atmosphere [2]. In addition to carbon emissions from the burning of fossil fuels such as oil and coal, CO_2 released by soil respiration is also an important source contributing to global warming [3,4].

Soils constitute the Earth's largest terrestrial carbon pool [5–7]. Thus, small fluctuations in soil organic carbon will largely influence atmospheric CO_2 concentrations and change the global carbon balance pattern [8]. Soil organic carbon stocks and fluxes are soil- and site-specific and reflect the long-term balance between organic matter inputs from vegetation and losses due to respiration, decomposition, erosion, and leaching.

Furthermore, SOC can affect the global biogeochemical cycle through coupling with nutrient elements such as nitrogen and phosphorus, thus affecting ecosystem processes [9,10]. Especially against the background of global climate change, the soil C cycle may significantly impact ecosystem productivity, biodiversity, and sustainable development through interactions with multiple drivers of global change, including increased CO_2 concentration, N deposition, climate warming, and land-use changes [11,12].

Therefore, studies on SOC inventories and their changes can provide a scientific and reliable basis for research on the global carbon cycle.

Studies have shown that SOC inventories are closely related to environmental variables such as climate, vegetation, and terrain [13–17]. Changes in environmental variables not only directly affect the density of SOC, but also play an important role in the spatial–temporal distribution pattern of SOC. Therefore, it is particularly important to reveal the driving forces behind changes in different environmental variables and their effects on SOC [18]. The relationship between SOC decomposition and climate factors—especially its sensitivity to temperature and precipitation—is now the focus of academic attention. Under the comprehensive influence of climate change and human activities, SOC inventories and dynamic balance will change. Thus, the SOC pool may serve as both a carbon sink and carbon source which, in turn, will influence global climate change.

The statistical analysis of the relationships between environmental variables and SOC inventories is of great significance for assessing the impact of future climate change on soil carbon pools [19]. Factors controlling SOC cycles differ under different environmental conditions; so, there is high spatial–temporal variability in SOC [20]. In this context, many research studies have been conducted [21–23]; however, most of them have focused on the spatial variation in SOC, while temporal variation—especially long-term monitoring—was seldom involved. In addition, linear regression methods are often used [24–29], especially the GWR method, which has achieved good results [30–32]. However, non-linear relationships may better describe the spatial variation in SOC [33–36], among which machine learning methods have shown great advantages, including random forests, support vector machines, regression trees, and neural networks [37–42].

The Global Geochemical Baselines (GGB) project aims to provide a long-term and effective quantitative scale for resource and environmental assessment. The GGB project divides the world into several grids of a certain size and collects representative samples to reflect the overall element levels of the grid [43,44]. As a part of the GGB project, the far-reaching China Geochemical Baselines (CGB) resource and environmental projects were completed in 2008–2012 (CGB I) and 2015–2019 (CGB II), respectively, using 81 geochemical parameters [45–47]. Guangdong Province is located in the southern coastal region of China, for which CGB I was implemented in 2009, and CGB II was implemented in 2016. In 2023, we re-sampled soils at the same sites to monitor long-term SOC changes. This study takes Guangdong Province, China, as the study area, aiming to identify the spatial–temporal variations in SOC over the past 14 years, quantify the driving factors using a random forest algorithm, and evaluate the SOC inventories in Guangdong Province. This study is of great significance for the in-depth understanding of SOC stabilization mechanisms and the carbon–climate feedback effect under global climate change. The generated research data are also important for carbon balance–global climate change simulation analysis and the formulation of climate change policies.

2. Materials

2.1. Introduction of Study Area

Guangdong Province is located in the southern coastal area of China, with an area of 17.97×10^4 km^2 (Figure 1). Its permanent population was 126.01 million in 2020, and its GDP was up to RMB 11,076.094 billion. It is the most populous and economically developed province in China. Guangdong Province has a subtropical monsoon climate, with high temperatures and rainy weather in the summer and relatively low temperatures and little rain in the winter. The average annual rainfall was 1801.08 mm, the average annual temperature was 22.3 °C, and the annual sunshine duration was 1705.6 h in 2020.

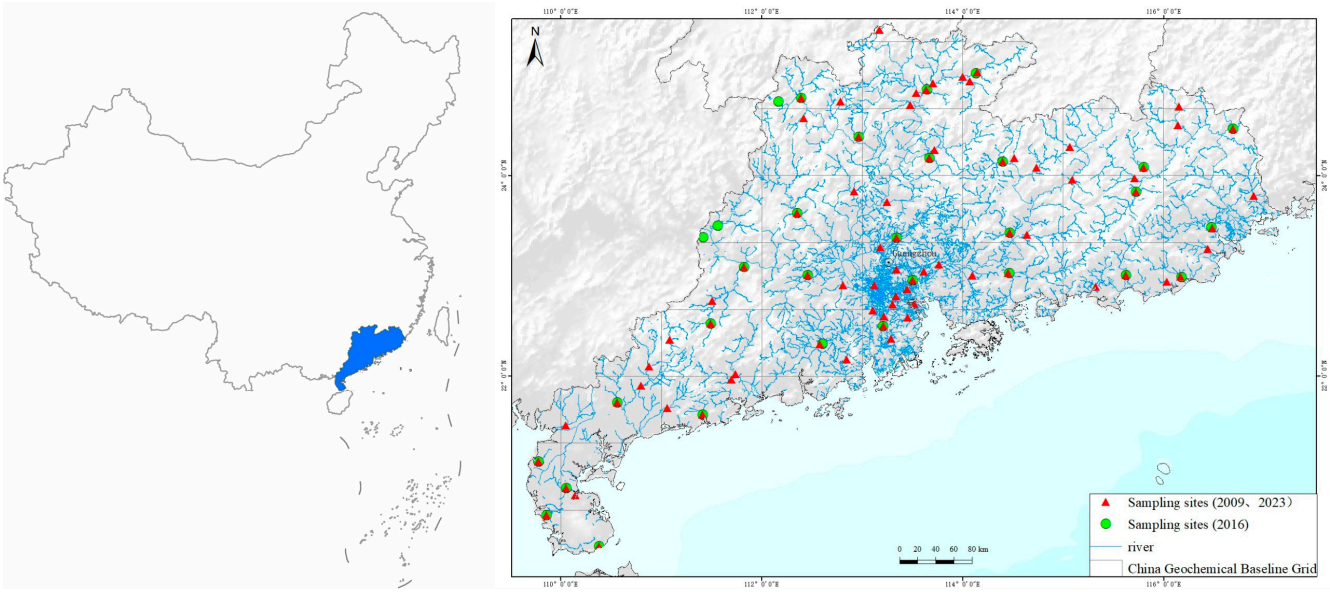

Figure 1. Study area and sampling sites.

The lithology of Guangdong Province is mainly granite, unconsolidated sediment, mixed sedimentary rocks, and carbonate rocks (Figure 2). Soil types in Guangdong Province are mainly Alisols, including Haplic Acrisols, Ferric Acrisols, and Humic Acrisols (Figure 3).

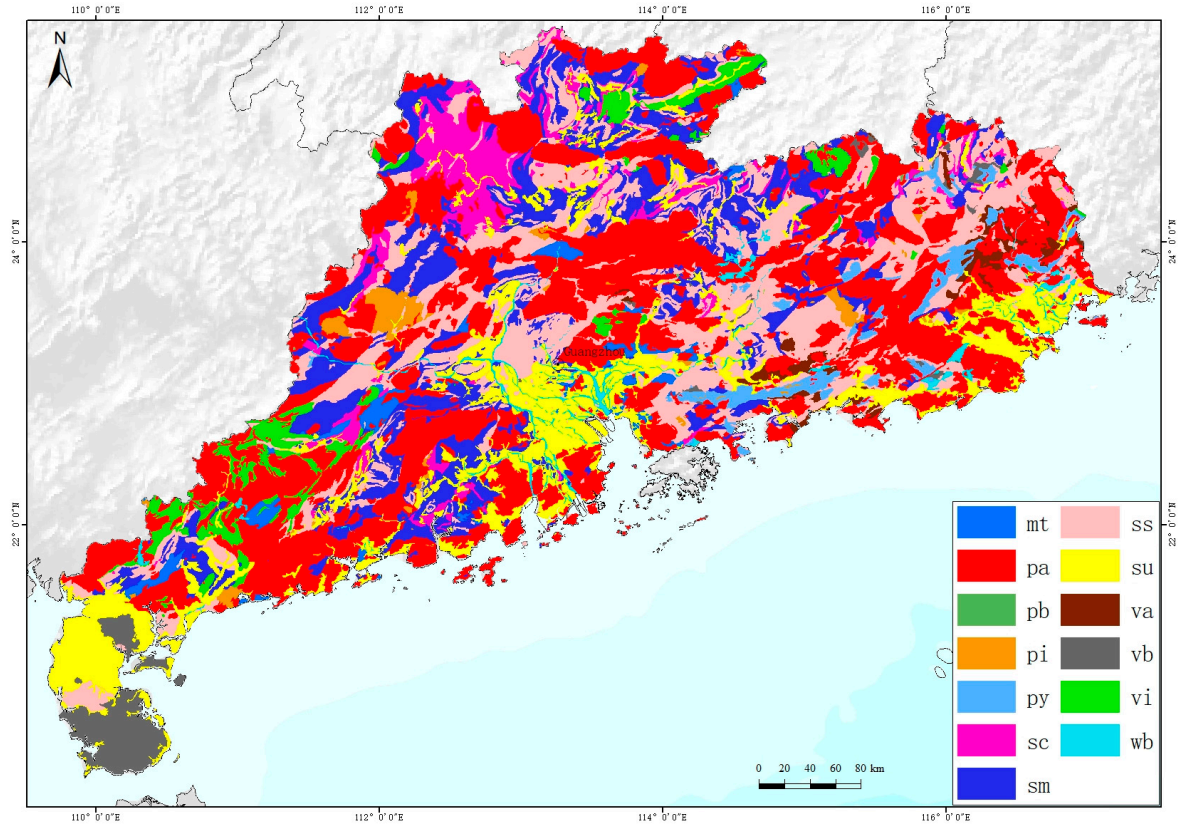

Figure 2. Geological map of Guangdong (mt: metamorphic rocks; pa: acid plutonic rocks; pb: basic plutonic rocks; pi: intermediate plutonic rocks; py: pyroclastics; sc: carbonate sedimentary rocks; sm: mixed sedimentary rocks; ss: siliciclastic sedimentary rocks; su: unconsolidated sediment; va: acid volcanic rocks; vb: basic volcanic rocks; vi: intermediate volcanic rocks; and wb: water body).

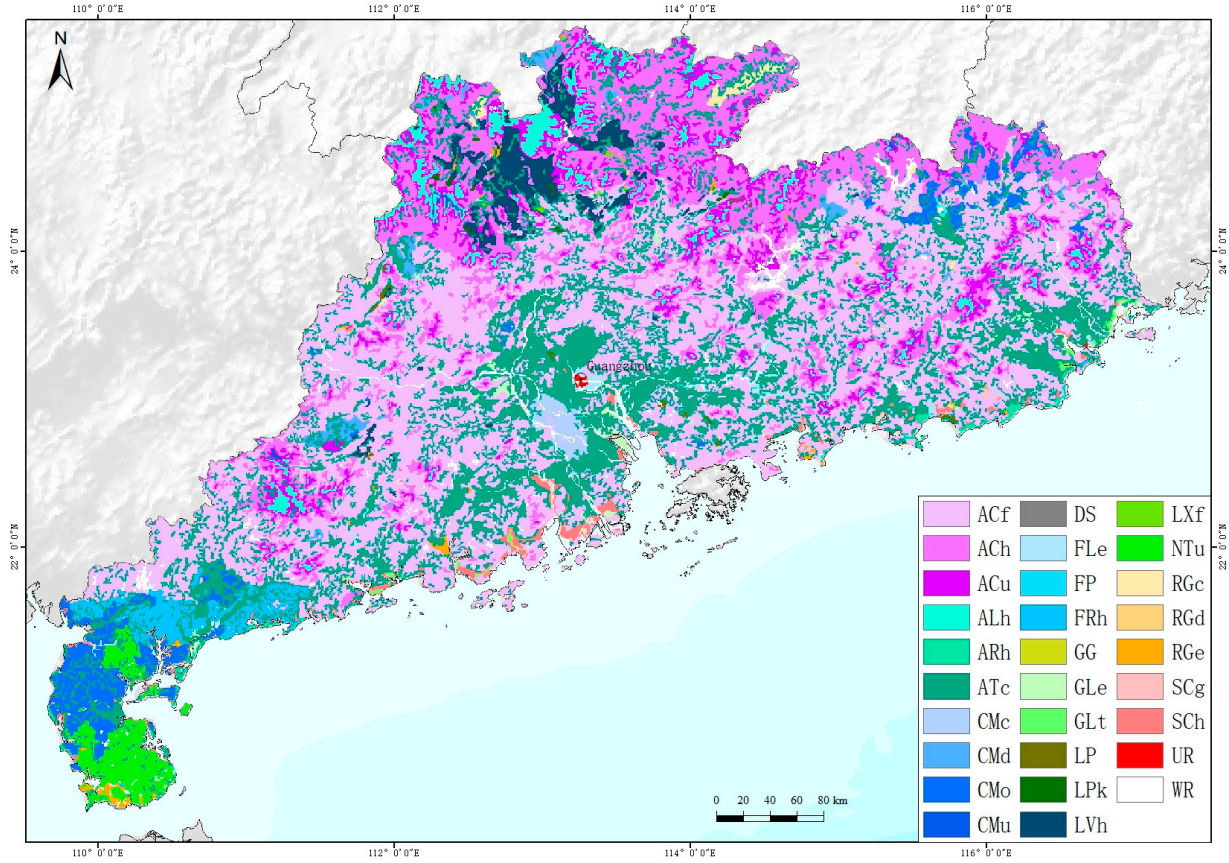

Figure 3. Soil types of Guangdong (ACf: Ferric Acrisols; ACh: Haplic Acrisols; ACu: Humic Acrisols; ALh: Haploc Alisols; ARh: Haplic Arenosols; ATc: Cumulic Anthrosols; CMc: Calcaric Cambisols; CMd: Dystric Cambisols; CMo: Ferralic Cambisols; CMu: Humic Cambisols; DS: Dunes&shift.sands; FLe: Eutric Fluvisols; FP: Fishpond; FRh: Haplic Ferralsols; GG: Glaciers; GLe: Eutric Gleysols; GLt: Thionic Gleysols; LP: Leptosols; LPk: Rendzic Leptosols; LVh: Haplic Luvisols; LXf: Ferric Lixisols; NTu: Humic Nitisols; RGc: Calcaric Regosols; RGd: Dystric Regosols; RGe: Eutric Regosols; SCg: Gleyic Solonchaks; SCh: Haplic Solonchaks; UR: Urban, mining, etc. and WR: Water Region).

2.2. Sample Collection

A total of 77 samples were collected in Guangdong Province in 2009 and 2023, with about 2–3 samples collected per sample grid, as well as 31 samples in 2016, with 1 sample per sample grid collected. Alluvial soils are the most representative sampling medium, which not only represent the mean value of elements in the whole basin, but also effectively reflect environmental changes. The elements released by the natural weathering of upstream rocks will be transported by surface water and deposited in the plains, deltas, floodplains, or basins in low-lying areas. Thus, the samples can represent the average value of the elements in the basin due to the mixing process during transporting. Almost all of the grids are controlled with samples; thus, the samples in each grid represent the average content within that grid (Figure 1). The sampling media, sampling methods, analytical laboratories and methods, and quality control were identical for CGB I and CGB II, making the data comparable.

2.3. Sample Analysis

All samples were air-dried either in a room or under shade, without exposure to sunlight, and sieved through a 2 mm nylon mesh screen. They were subsequently ground to <200 mesh in an agate or pure aluminum porcelain mill [46,48]. All samples were analyzed in the laboratory of the Institute of Geophysical and Geochemical Exploration, Chinese Academy of Geological Sciences. The SOC content was determined using a high-

frequency infrared absorption method. Additionally, 50% hydrochloric acid was used to remove carbonate interference during sample pre-treatment. During the analysis, the soil samples were heated to over 800 °C in an oxygen-rich environment, and the SOC was oxidized to CO_2. The resulting CO_2 was fed into a non-dispersive infrared detector, and the SOC content was calculated based on the intensity of CO_2 absorption. All chemical analyses performed during the CGB project were conducted under strict quality control measures, which have been described in detail in [45]. Analytical accuracy and precision were controlled based on analyses of standard reference materials as well as field and laboratory replicate samples. The analysis methods and detection limits are detailed in Table 1.

Table 1. Analysis methods and detection limits.

Index	Analysis Method	Detection Limits	Units
SiO_2	X-ray fluorescence spectrometry	0.1	%
Al_2O_3	X-ray fluorescence spectrometry	0.05	%
TFe_2O_3	X-ray fluorescence spectrometry	0.05	%
FeO	X-ray fluorescence spectrometry	0.1	%
MgO	Plasma emission spectrometry	0.05	%
CaO	X-ray fluorescence spectrometry	0.05	%
SOC	High-frequency combustion—infrared carbon sulfur meter	0.1	%

2.4. Environmental Covariates

Soil parent material, soil type, climate (mean annual temperature, mean annual precipitation), NDVI (normalized difference vegetation index), vegetation type, and land-use type (LUCC) were taken as the environmental covariates which may control the change in SOC. The parent material data were obtained from the Geological map of Guangdong Province [49]. The climate data (mean annual temperature, mean annual precipitation) and NDVI were obtained from the Resources and Environmental Sciences and Data Center of Chinese Academy of Sciences, comprising mean annual data (https://www.resdc.cn/data.aspx?DATAID=123, accessed on 6 March 2023). Normalized difference vegetation index (NDVI) data at a 30 m spatial resolution were calculated using bands 4 (red) and 5 (near infrared) of Landsat 8 images collected from the image inventory of USGS Earth Explorer using the maximum value synthesis method.

2.5. Estimate of SOC Inventories

The SOC density (SOCD) is a necessary indicator of soil properties for calculating SOC inventories. The SOCD can be determined according to the SOC content and BD, and was calculated using the following equation [19]:

$$SOCD = SOC \times BD \times H \times 10^{-1},$$

where SOCD represents the SOC density (kg/m^2), BD represents soil bulk density (g/cm^3), and H represents soil thickness (cm).

The SOCI was calculated using the following equation:

$$SOCI = SOCD \times S \times 10^{-3},$$

where SOCI represents SOC Inventories (t), SOCD represents the SOC density(kg/m^2), and S represents the soil area (m^2).

2.6. Random Forest

The random forest algorithm is a classical combined classifier algorithm, proposed in [50]. A bagging algorithm is used to generate training sample subsets and a classification regression tree is used as a meta-classifier. Candidate attributes are randomly selected to

split the current node when building a single cart tree. This doubly random (with respect to both the training set and attributes) strategy results in greater differences between the meta-classifiers, which makes the random forest algorithm perform better in classification [51].

The random forest algorithm is a combination of tree classifiers {h(x,θk), k = 1, ...}, where the meta-classifier h(x,θk) is a complete growth and non-pruning classification regression tree, x is the input vector, and θk is an independent and identically distributed random vector, which determines the growth process of a single classification regression tree. For classification, the output of the random forest algorithm is the result of simple majority voting and, for regression, the output is the simple average of the output of a single tree.

The random forest approach presents many advantages; for example, the algorithm can deal with both continuous and category attributes through the use of the cart algorithm as its meta-learning algorithm. Moreover, the decision tree allows for greater differences and better classification performance, due to the combination of the bagging algorithm and randomly selected candidate feature splitting, which prevents over-fitting and tolerance to noise.

Another prominent feature of the random forest algorithm is the calculation of the importance of variables. First, the random forest algorithm adds disturbances through the random re-ordering of the variables of training samples, following which the change in the classification accuracy of all samples in the decision tree is observed before and after disturbance, in order to measure the importance of the variables.

The random forest analysis was completed in R4.2.2 [52].

2.7. Prediction Method of SOC Inventories

We used the ArcGIS resample tool to divide Guangdong Province into 19,300 3 km × 3 km grids, and the attributes of environmental covariates (including temperature, precipitation, NDVI, soil type, and soil parent material) were extracted for each grid. Then, the SOC content of each grid was predicted using the random forest algorithm, according to the environmental covariates. Finally, the SOC inventories in Guangdong Province were calculated using ArcGIS 10.8.

2.8. Accuracy of SOC Inventories Prediction

A cross-validation approach [53] was used to assess the accuracy of predicted SOC stocks. Cross-validation—also referred to as the "leave-one-out validation approach"—removes one observation and estimates the value of SOC stocks at that location with the remaining observations. The root mean square error (RMSE) was computed to assess the prediction accuracies of all three predictions:

$$RMSE = \sqrt{\frac{1}{n}\sum_{i=1}^{n}[SOC_{me}(x_i) - SOC_{es}(x_i)]^2}$$

where $SOC_{me}(x_i)$ is the measured SOC, $SOC_{es}(x_i)$ is the estimated SOC at the ith location, and n is the number of validation predictions.

3. Results

3.1. Summary Statistics of SOC Content

The mean and median values of SOC in Guangdong Province were 0.81% and 0.71% in 2009; 1.13% and 0.95% in 2016; and 1.02% and 0.95% in 2023, respectively. The mean value of SOC in 2009 was lower than that for China overall; in contrast, both the mean and median values of SOC in 2016 were higher than that for China (Table 2). The mean value of SOC in Guangdong Province in 2016 was higher than those in 2009 and 2023, and moreover with a large coefficient of variation.

Table 2. Descriptive statistical characteristics of SOC.

	Min	Mean	Median	Max	CV	N
Guangdong 2009	0.163	0.808	0.707	2.639	56.42	76
Guangdong 2016	0.253	1.128	0.945	2.902	57.65	31
Guangdong 2023	0.149	1.017	0.947	2.768	52.29	76
China 2009	0.006	0.865	0.601	11.360	110.19	3382
China 2016	0.006	0.904	0.688	6.843	96.66	1690

Unit: %; CV: coefficient of variation; N: number of samples; data of SOC for China 2009 and China 2016 were from Global Geochemical Baselines (GGB) project [43,45,46].

3.2. Soil Organic Carbon Content in Soils Developed from Different Parent Materials

The SOC in soils developed from different parent materials was counted and a histogram was drawn, as shown in Figure 4. The results indicated that, in 2009, the SOC contents in soils developed from carbonate rocks was the highest, with a mean value of 1.35%, followed by unconsolidated sediments and basic volcanic rocks, with mean values of 0.87% and 0.81%, respectively, while the organic carbon contents in granite-developed soils was the lowest. In 2016, the organic carbon content in soils developed from basic volcanic rocks was the highest, with an average value of 1.36%, followed by mixed sedimentary rocks and unconsolidated sediment-developed soils, with average values of 1.21% and 1.20%, respectively, while the organic carbon contents in soils developed from granite was the lowest. In 2023, the SOC content in soils developed from carbonate rocks was the highest, with an average value of 1.44%, while those in soils developed from granite and basic volcanic rocks were the lowest.

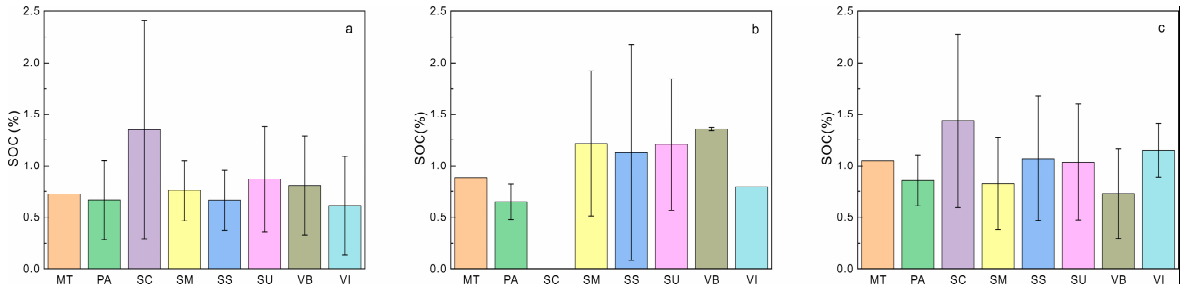

Figure 4. SOC content in soils developed from different parent materials: (**a**) 2009; (**b**) 2016; and (**c**) 2023. MT: metamorphic rocks; PA: acid plutonic rocks; SC: carbonate sedimentary rocks; SM: mixed sedimentary rocks; SS: siliciclastic sedimentary rocks; SU: unconsolidated sediment; VB: basic volcanic rocks; and VI: intermediate volcanic rocks. The error bars represent standard deviations.

The SOC was significantly different in soils developed from different parent materials and at different sampling times. Overall, the SOC in soils developed from carbonate rock was the highest, followed by unconsolidated sediments, while that for soil developed from granite was the lowest.

3.3. Soil Organic Carbon Content in Different Soil Types

The soil organic carbon content in different soil types was counted and a histogram was drawn, as shown in Figure 5. The results showed that, in 2009, the SOC contents in Haplic Luvisols, Calcaric Cambisols, and Eutric Gleysols were higher (1.40%, 1.25%, and 1.23%, respectively), while those in Dystric Cambisols and Calcaric Cambisols were relatively lower. In 2016, the SOC contents in Cumulic Anthrosols, Ferralic Cambisols, and Calcaric Regosols were higher, with averages of 1.45%, 1.41%, and 1.35%, respectively. In 2023, Haplic Luvisols, Calcaric Cambisols, and Haplic Acrisols had higher organic carbon contents, the mean values of which were 1.32%, 1.26%, and 1.36%, respectively. The SOC in different soil types was similar in 2009 and 2023, while that in 2016 was significantly

different. The SOC contents of Eutric Gleysols, Haplic Luvisols, and Calcaric Cambisols were relatively high overall.

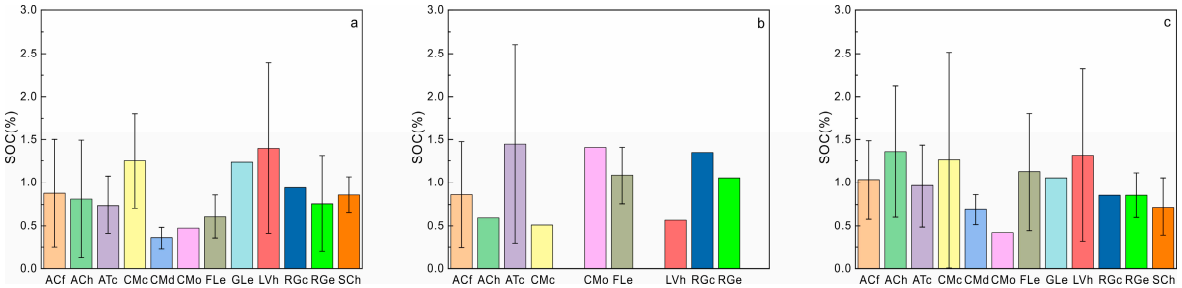

Figure 5. SOC content in different soil types: (**a**) 2009; (**b**) 2016; and (**c**) 2023. ACf: Ferric Acrisols; ACh: Haplic Acrisols; ATc: Cumulic Anthrosols; CMc: Calcaric Cambisols; CMd: Dystric Cambisols; CMo: Ferralic Cambisols; FLe: Eutric Fluvisols; GLe: Eutric Gleysols; LVh: Haplic Luvisols; RGc: Calcaric Regosols; RGe: Eutric Regosols; and SCh: Haplic Solonchaks. The error bars represent standard deviations.

3.4. Correlations between SOC and Oxides

The correlations between SOC and major oxides are shown in Figure 6. The results indicate that, in 2009, SOC was significantly positively correlated with FeO, Al_2O_3, MgO, and CaO, with correlation coefficients of 0.78, 0.5, 0.45, and 0.43, respectively. In 2016, soil organic carbon showed significant positive correlations with FeO and Fe_2O_3, with correlation coefficients of 0.82 and 0.63, respectively. Compared with 2009, the correlation coefficient with FeO increased, while that with Fe_2O_3 decreased slightly; there were also positive correlations with MgO and CaO, where the correlation coefficients were 0.48 and 0.39, respectively. In 2023, there were significant positive correlations between soil organic carbon and FeO and Al_2O_3, with correlation coefficients of 0.9 and 0.43, respectively.

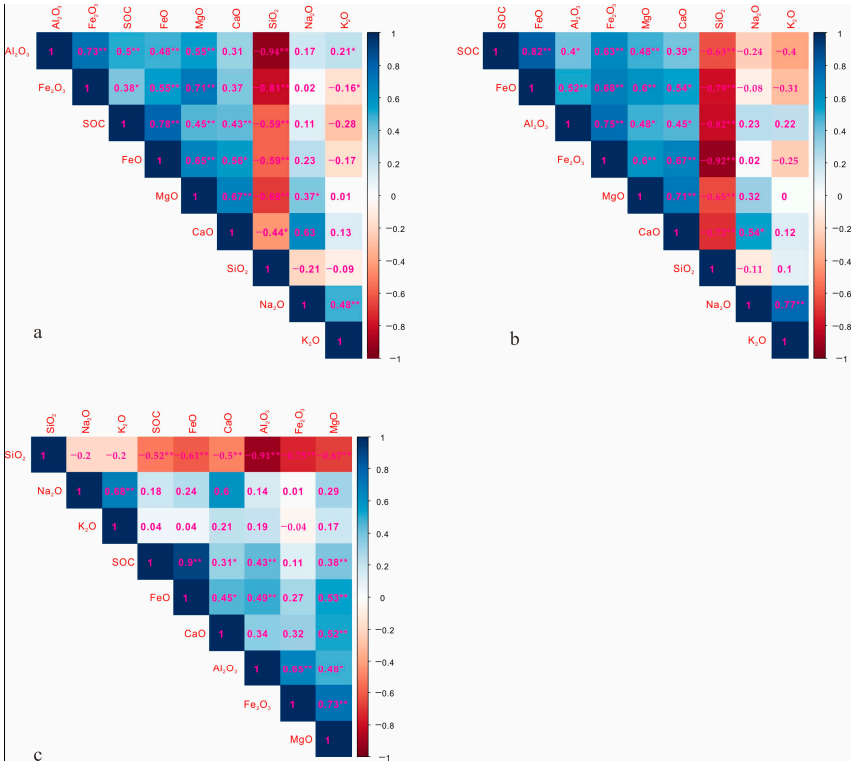

Figure 6. Correlations between soil organic carbon and oxides: (**a**) 2009; (**b**) 2016; and (**c**) 2023. **: significantly correlated at the 0.01 level; *: significantly correlated at the 0.05 level.

3.5. Spatial Variations in SOC

In 2009, the SOC in Guangdong Province was relatively low overall, and the high-valued areas were mainly distributed in Zhuhai, Zhongshan, and the north of Qingyuan and Meizhou. In 2016, the SOC in Guangdong Province increased significantly, and the spatial distribution pattern was significantly different from that in 2009. Zhanjiang in western Guangdong showed obvious high SOC values, while soils in the Pearl River Delta, Qingyuan City, and northern Zhaoqing, Meizhou, and Shantou also presented high organic carbon contents. In 2023, the soils with high SOC concentrations were mainly located in Guangzhou, Zhongshan, Zhuhai, northern Meizhou, and Shaoguan (Figure 7).

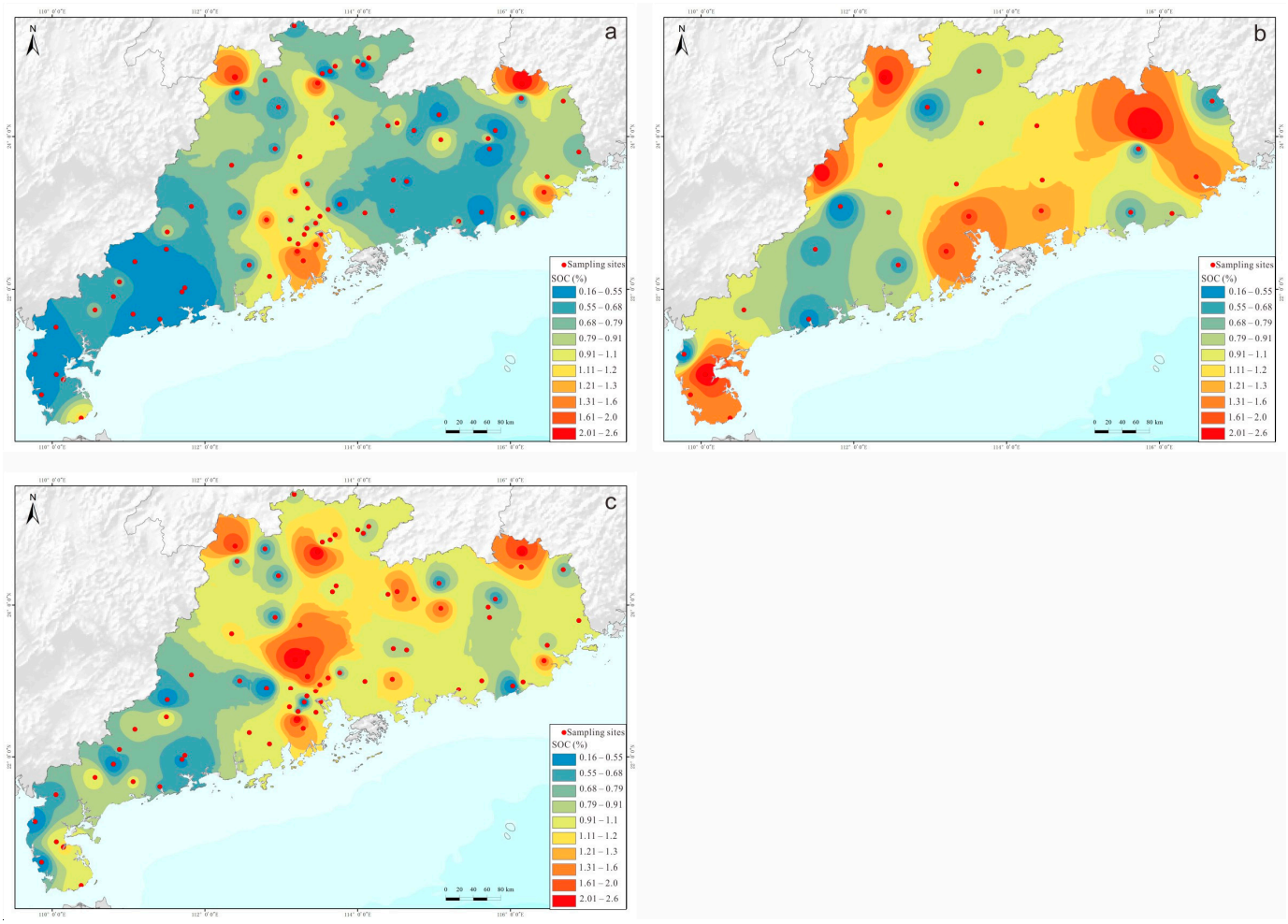

Figure 7. Geochemical map of SOC in Guangdong Province: (**a**) 2009; (**b**) 2016; and (**c**) 2023.

3.6. Model Performance and Drivers of SOC

The random forest regression model explained 44.8% (R^2) of SOC concentration variability across all sites in 2009, 36.2% for 2016, and 41.1% for 2023, suggesting that about 40% of the spatial variability of SOC was explained by soil parent materials, soil type, precipitation, NDVI, temperature, land-use type, and vegetation type. The root mean square error (RMSE = 0.14% for 2009, 0.13% for 2016 and 2023) indicated an acceptable prediction accuracy. The random forest model revealed that the three most important predictors of SOC spatial distribution were temperature, precipitation, and NDVI. The remaining predictors showed lower, but non-negligible, influences (Figure 8).

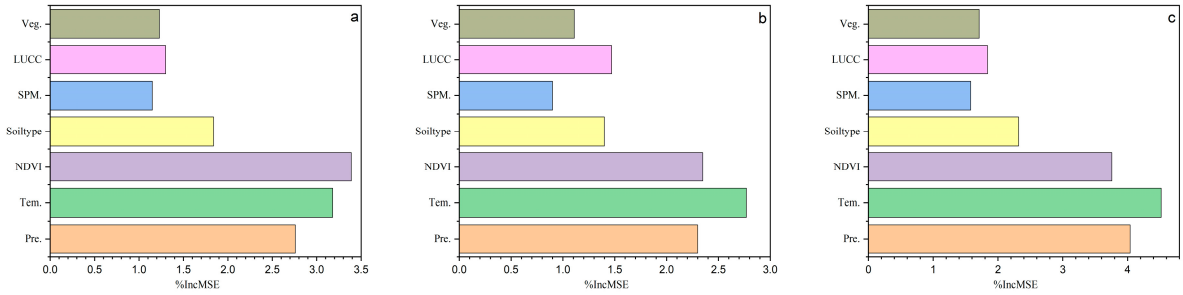

Figure 8. Influencing factors of spatial variation in SOC in Guangdong Province: (**a**) 2009; (**b**) 2016; and (**c**) 2023. Veg.: vegetation type; LUCC: land-use type; SPM.: soil parent material; Tem.: temperature; and Pre.: precipitation.

3.7. Prediction of SOC Density and Inventories

The SOC density and inventories in Guangdong Province were calculated, and the results predicted using the random forest method are shown in Figure 9. In 2009, the areas with high SOC contents in Guangdong Province were mainly distributed in the northern parts of Guangdong, Zhongshan, and Zhuhai. In 2016, SOC in Guangdong increased significantly, and the high-value areas were mainly distributed in Zhanjiang, Foshan, and Zhongshan in the Pearl River Delta, as well as parts of northern and eastern Guangdong Province. In 2023, the SOC content decreased significantly, and the high-valued areas mainly appeared in parts of northern and eastern Guangdong Province.

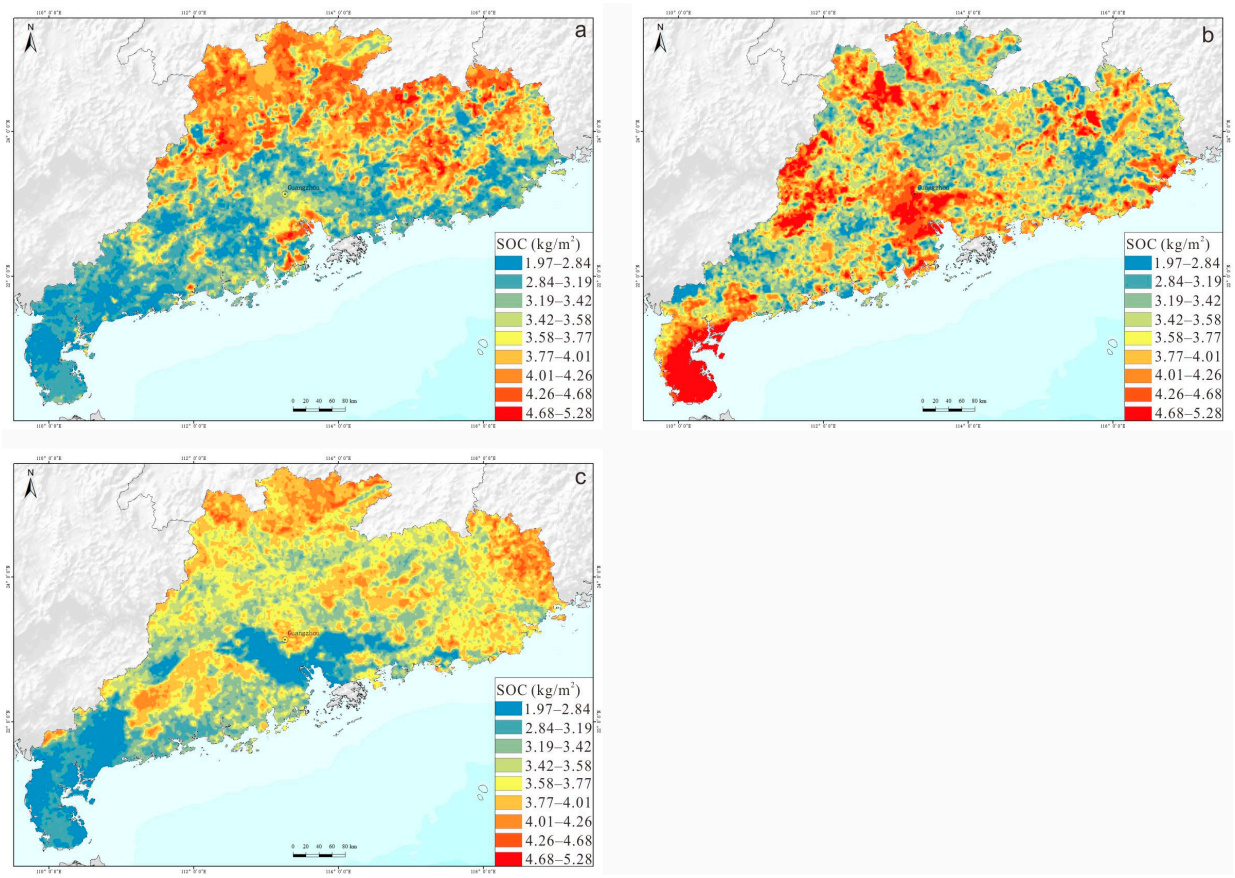

Figure 9. Prediction of SOC density in Guangdong Province: (**a**) 2009; (**b**) 2016; and (**c**) 2023.

As shown in Table 3, the average SOC density in Guangdong in 2009 was 3.1 kg/m^2, while it was 4.34 kg/m^2 in 2016, and 3.94 kg/m^2 in 2009. The SOC inventories in topsoils (0–30 cm) in Guangdong were 0.61 Pg in 2009, 0.74 Pg in 2016, and 0.62 Pg in 2023 (Figure 10).

Table 3. Statistical analysis of SOC density in surface soils (0–30 cm) of Guangdong Province (kg/m^2).

Year	Min	Mean	Median	Max
2009	0.63	3.14	2.75	10.25
2016	0.98	4.38	3.67	11.27
2023	0.58	3.95	3.68	10.75

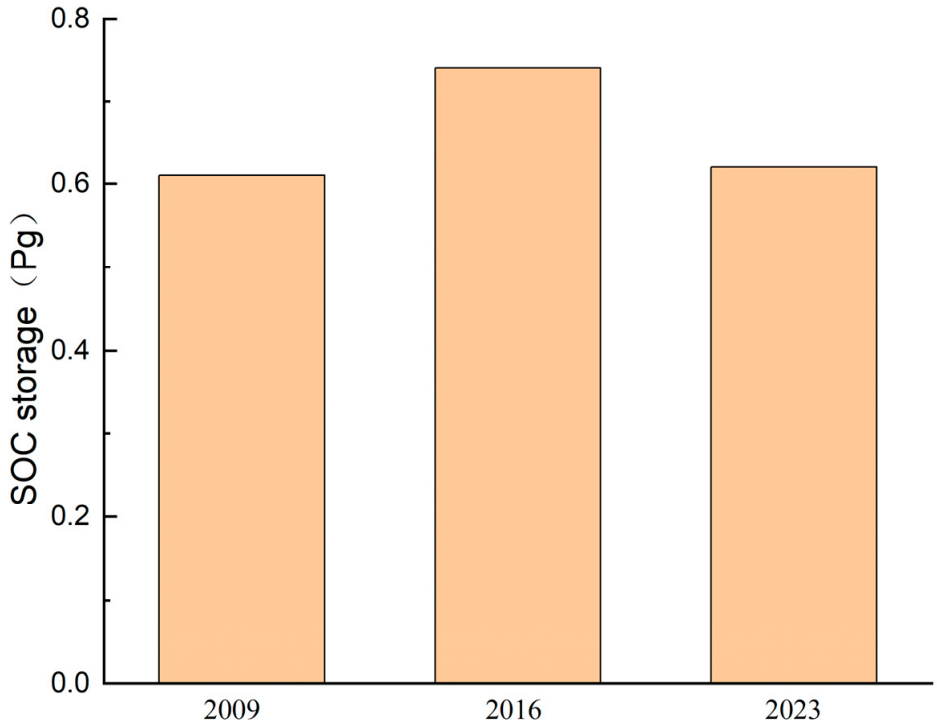

Figure 10. Soil organic carbon inventories in Guangdong Province.

3.8. Temporal Variation in SOC

Overall, the soil of Guangdong Province acted as a carbon sink from 2009 to 2016, among which Zhanjiang in western Guangdong, parts of Maoming in eastern Guangdong, and most parts of the Pearl River Delta appear to be high carbon sinks. There were also some areas that acted as carbon sources, mainly distributed in the eastern part of northern Guangdong (Figure 11a). From 2016 to 2023, the soil in Guangdong Province mostly acted as a carbon source, and the SOC contents in Zhanjiang and Maoming in western Guangdong and Zhongshan, Jiangmen, Zhaoqing, and Dongguan in the Pearl River Delta decreased significantly, while parts of northern and eastern Guangdong appeared to be carbon sinks (Figure 11b). From the perspective of the period 2009–2023, soil organic carbon in Guangdong Province acted as a carbon source, and carbon sink areas were distributed in a scattered manner, while soils in Dongguan, Zhongshan, Zhuhai, and Shenzhen in the Pearl River Delta were obvious carbon sources (Figure 11c).

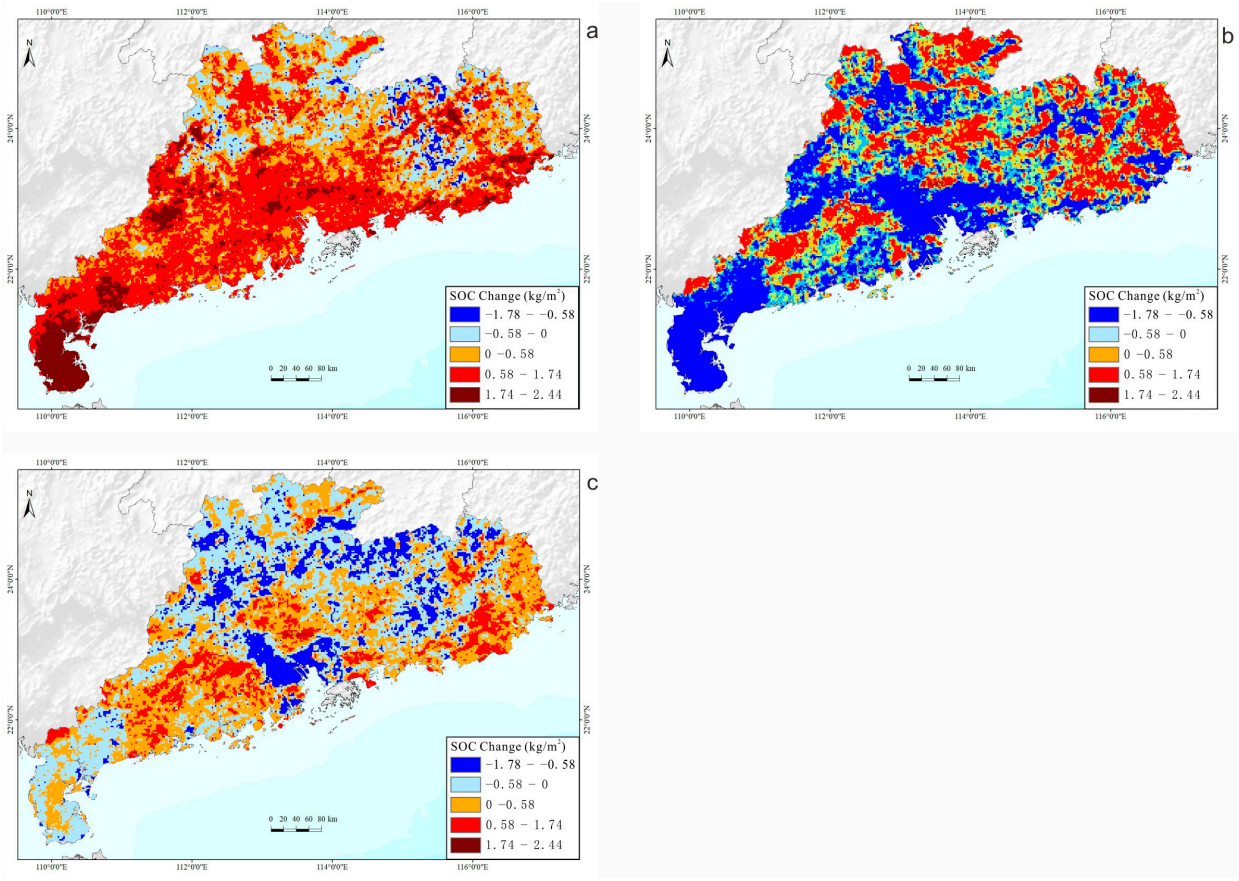

Figure 11. Change in SOC density in Guangdong Province: (**a**) 2009–2016; (**b**) 2016–2023; and (**c**) 2009–2023.

4. Discussion

4.1. Stabilization Mechanism of SOC

The stabilization mechanism of SOC determines the ability of soil to fix and store organic carbon [54–58]. At present, there is increasing evidence that the stability of SOC may depend on complex interactions between organic carbon and minerals [59], such as the formation of organic–inorganic complexes with iron and aluminum oxides, which control SOC stability over a longer time scale [60–62]. Studies have shown that about 90% of long-term SOC inventories are closely related to soil minerals [63]. Soil organic carbon binds to minerals through ligand exchange, cation bridge, the van der Waals force, or hydrogen bonding, and organic macromolecules are adsorbed onto mineral surfaces to form organic–inorganic complexes [64,65]. The interaction between organic carbon and metal ions on mineral surfaces greatly enhances the stability of organic carbon [66,67].

Therefore, the high organic carbon content of basalt-developed soils may be closely related to the large amount of iron oxides, while the retention of SOC in soil developed from carbonate rocks is related to calcium oxide and magnesium oxides. SOC can be adsorbed onto the surface of metal minerals in a variety of forms, reducing the contact between SOC and micro-organisms or biological enzymes and, thus, avoiding self-degradation. The formation of organic–mineral complexes can prevent microbial decomposition and effectively maintain the stability of SOC [68]. In the stabilization process of SOC, metal minerals—especially iron minerals—play a significant role. The iron minerals, characterized by a large specific surface area and strong adsorption capacity, can combine with SOC by means of precipitation and adsorption to maintain the stability of SOC [69]. In contrast, granite-developed soils contain less organic carbon, which may be due to the low contents of iron oxide, calcium oxide, or magnesium oxide, thus weakening the protective effect of soil minerals.

4.2. Prediction of SOC Inventories

Luo [70] evaluated the spatial distribution of organic carbon density using 211 soil profiles collected in Guangdong Province in 2010. The spatial distribution of SOC density showed a significant spatial similarity with the predicted SOC density for 2009 in our research, suggesting that the prediction of SOC density in this research is reliable. Due to the high spatial variability of SOC, it is difficult to capture this spatial variability using traditional geochemical maps, which brings great uncertainty to the results. In contrast, the spatial variation characteristics of SOC can be more accurately inferred through combining environmental variables and quantitative models.

4.3. Influencing Factors of Temporal–Spatial Variation in SOC

We plotted the temperature, precipitation, and NDVI maps of Guangdong Province (Figure 12). The regional difference in SOC density for Guangdong Province was found to be closely related to the difference in hydrothermal conditions between the north and south regions of the province. Generally speaking, from south to north, with the decrease in temperature and rainfall, the intensity of leaching and mineralization of organic matter gradually weakens (in most cases, such as 2009 and 2023; 2016 is an exception, due to extreme weather conditions). In addition, as northern Guangdong is a mountainous area with dense vegetation cover and less human disturbance, vegetation is a direct factor affecting soil organic carbon content.

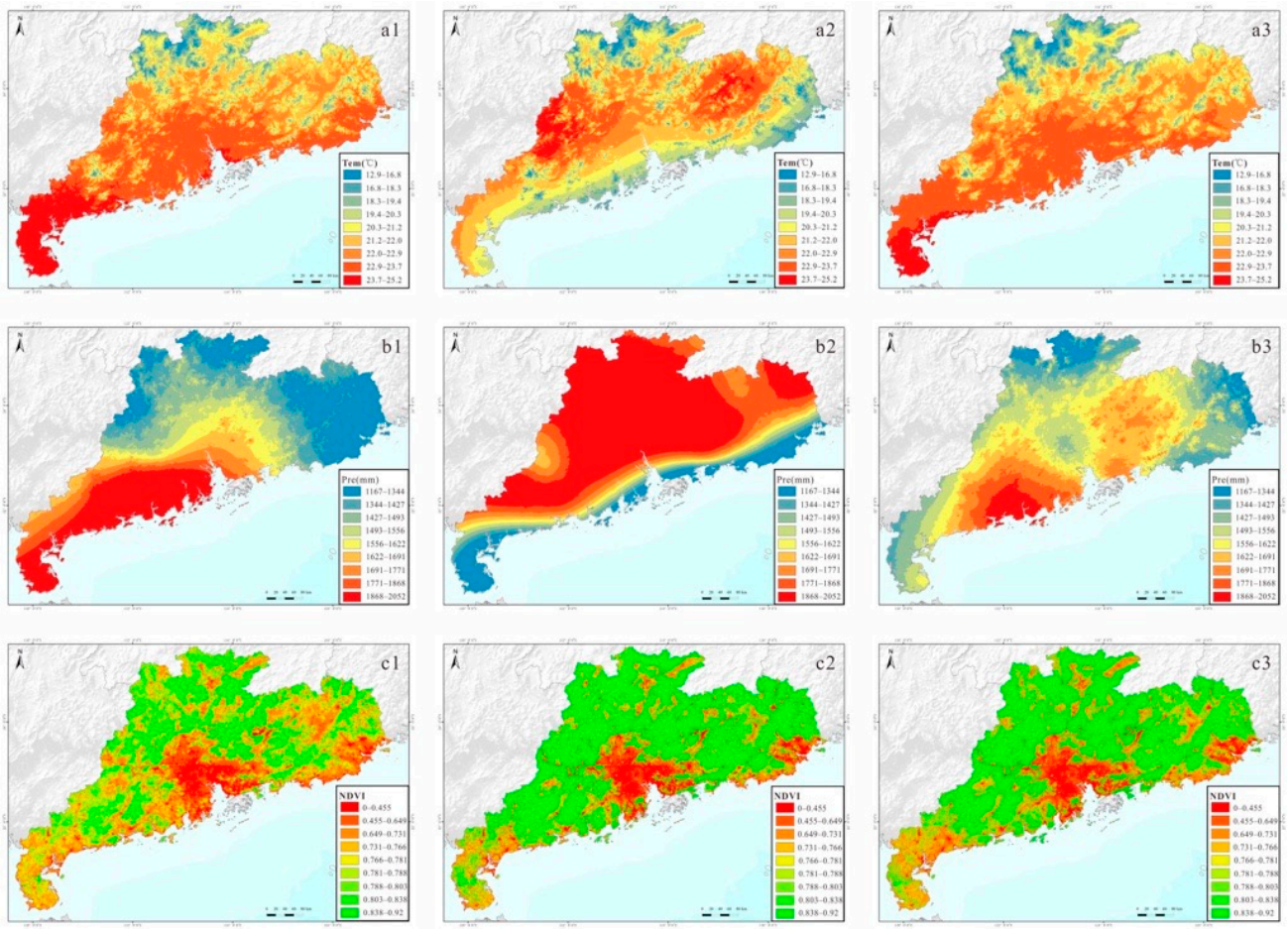

Figure 12. Environmental covariates in Guangdong: (**a1**) temperature 2009; (**a2**) temperature 2016; (**a3**) temperature 2022; (**b1**) precipitation 2009; (**b2**) precipitation 2016; (**b3**) precipitation 2022; (**c1**) NDVI 2009; (**c2**) NDVI 2016; and (**c3**) NDVI 2022.

Soil fixes organic carbon through the decomposition and transformation of carbon dioxides by plant photosynthesis, and releases carbon dioxide into the air through soil respiration. Soil organic carbon stocks and fluxes are soil- and site-specific and reflect the long-term balance between the two. The NDVI is an indicator of primary and ecological productivity [71]. The average value of the NDVI was 0.746 in 2009, 0.786 in 2016, and 0.777 in 2022, suggesting that the SOC input in 2016 was the highest. Deng [72] evaluated the temporal and spatial changes in vegetation carbon sequestration in Guangdong Province and found that the vegetation carbon sequestration in 2016 was significantly higher than that in 2009—the same result as our research. The average temperatures in 2009 and 2023 were 22 °C and 21.8 °C, respectively, and the spatial variation in temperature between the two was similar, showing a trend of low temperature in the north and high temperature in the south. However, the temperature pattern in 2016 was different from the other two years, with an annual average temperature of 21.2 °C, showing the lowest temperature relative to 2009 and 2023. Moreover, the temperature in the southeast coast region was significantly lower in 2016, especially for Leizhou Peninsula, where the temperature was higher in 2009 and 2023. In 2009 and 2023, the rainfall in Guangdong Province showed a trend of low in the north and high in the south, with an average annual rainfall of 1597 mm and 1567 mm, respectively, while the rainfall in 2016 increased significantly, with an average of 1869 mm, showing a very different spatial distribution from that of 2009 and 2023: high in the north and low in the south, with a rare drought occurring in the southeast coast region.

In general, temperature is considered to be the main factor affecting soil respiration. Most studies have found that global soil respiration increases significantly under global warming. At the physiological and biochemical level, temperature is necessary to regulate the breakdown of enzymes needed for respiration. At the ecosystem level, the supply of respiration substrates to the subsurface parts of the plant is also driven by temperature, which has an impact on soil respiration. Temperature is a significant driving force for the variation in soil respiration, due to its influence on the adsorption and desorption of soil organic matter and mineral surface, as well as its direct effects on the activities of micro-organisms and soil enzymes [73,74].

Precipitation can increase soil moisture in farmland, promote crop growth, increase crop productivity and, thus, increase soil carbon input. Moreover, precipitation promotes microbial activity and improves soil respiration [3], thereby increasing the soil carbon output. The effect of precipitation on carbon sequestration in farmland ecosystems depends on the balance between these two factors. The relationship between annual precipitation and surface SOC content is complex. Generally speaking, when precipitation is between 400 and 900 mm, SOC decreases with increasing precipitation; meanwhile, when the precipitation is greater than 900 mm, SOC increases with increasing precipitation. However, the influence of precipitation on soil respiration is also affected by the instantaneous intensity and frequency of rainfall [75].

The most typical change in SOC source and sink was observed in Leizhou Peninsula, where extreme climate conditions led to a severe low-temperature drought in 2016, compared with previous years (from 2009 to 2016, the average temperature in Leizhou Peninsula dropped from 24 °C to 20 °C, while the average precipitation dropped from 2400 mm to 1200 mm), and soil organic carbon mineralization decreased significantly, resulting in the rapid accumulation of SOC.

4.4. Limitations and Uncertainties

All of the data in this research were obtained from the China Geochemical Baseline Project. Alluvial soil samples were collected according to Global Reference Network grid cells for the whole of mainland China. The sampling media, sampling methods, analytical laboratories and methods, and quality control were all the same for CGB I and CGB II, making the data comparable. However, two to three samples per sample grid were collected for CGB I, while one sample per sample grid was collected for CGB II, resulting in thirty-one

samples for Guangdong Province with a limited sample size for CGB II relative to CGB I, which may have influenced the statistical results, to some extent. In addition, we did not consider the impacts of human activities on soil organic carbon storage in terrestrial ecosystems. It would be ideal if we could conduct future research at a more detailed level, for example, by taking more anthropogenic factors, such as vegetation and land-use types, into consideration.

5. Conclusions

The purpose of this study was to identify the spatial–temporal variations in SOC over the past 14 years (2009–2023) and quantify the main driving factors of spatial–temporal variations in soil organic carbon in Guangdong, China. The organic carbon contents in soils developed from different parent materials significantly differed. Overall, SOC in carbonate-developed soils was the highest, followed by basic volcanic rocks and unconsolidated sediment-developed soils, while that in granite-developed soils was the lowest. Therefore, soil minerals—especially iron- and calcium-based minerals—may play significant roles in soil organic carbon stabilization. The formation of organic–mineral complexes can prevent microbial decomposition and effectively maintain the stability of SOC.

The SOC inventories (0–30 cm) in Guangdong Province were 0.61 Pg in 2009, 0.74 Pg in 2016, and 0.62 Pg in 2023. From 2009 to 2016, soil organic carbon in Guangdong was mainly represented as a carbon sink, from 2016 to 2023 as a carbon source, and from 2009 to 2023 overall as a carbon sink. In Guangdong Province, the biggest changes in SOC were mainly distributed in Leizhou Peninsula and the Pearl River Delta. Finally, at the provincial scale in Guangdong, the most important driving force of spatial–temporal variations in SOC was temperature, followed by precipitation and NDVI.

Author Contributions: Conceptualization, M.T.; methodology, M.T.; software, M.T.; formal analysis, M.T.; investigation, C.W., Q.H., X.W., B.S., J.Z., Q.C., H.L., Y.L., J.Y. and X.L.; resources, C.W. and X.Z.; data curation, M.T., C.W. and W.W.; writing—original draft preparation, M.T.; writing—review and editing, M.T. and C.W.; visualization, C.W. and Q.H.; supervision, B.S. All authors have read and agreed to the published version of the manuscript.

Funding: This work was supported by 1:250,000 Regional Geochemical Survey of Eastern Guangdong and Integration of Provincial Results: (2024-16), National Natural Science Foundation (41907290), China Geological Survey Project (DD20221807), and Chemical Earth (GEO WP23_35, UNESCO 37/33).

Acknowledgments: We thank all members of the CGB sampling team.

Conflicts of Interest: The authors declare no conflicts of interest.

References

1. Davidson, E.A.; Trumbore, S.E.; Amundson, R. Biogeochemistry-soil warming and organic carbon content. *Nature* **2000**, *408*, 789–790. [CrossRef]
2. Houghton, J.T. Climate change 2001: The scientific basis. *Neth. J. Geosci.* **2001**, *87*, 197–199.
3. Raich, J.W.; PoRer, C.S. Global patterns of carbon dioxide emissions from soils. *Glob. Biogeochem. Cycles* **1995**, *9*, 23–36. [CrossRef]
4. Eswaran, H.; Van Den Berg, E.; Reich, P. Organic-carbon in soils of the world. *Soil Sci. Soc. Am. J.* **1993**, *57*, 192–194. [CrossRef]
5. Post, W.M.; Emanuel, W.R.; Zinke, P.J.; Stangenberger, A.G. Soil carbon pools and world life zones. *Nature* **1982**, *298*, 156–159. [CrossRef]
6. Batjes, N.H. Total carbon and nitrogen in the soils of the world. *Eur. J. Soil Sci.* **1996**, *47*, 151–163. [CrossRef]
7. Bohn, H.L. Estimate of organic-carbon in world soils. *Soil Sci. Soc. Am. J.* **1982**, *46*, 1118–1119. [CrossRef]
8. Stocker, B.D.; Roth, R.; Joos, F.; Spahni, R.; Steinacher, M.; Zaehle, S.; Bouwman, L.; Ri, X.; Prentice, I.C. Multiple greenhouse-gas feedbacks from the land biosphere under future climate change scenarios. *Nat. Clim. Chang.* **2013**, *3*, 666–672. [CrossRef]
9. Neff, J.C.; Townsend, A.R.; Gleixner, G.; Lehman, S.J.; Turnbull, J.; Bowman, W.D. Variable effects of nitrogen additions on the stability and turnover of soil carbon. *Nature* **2002**, *419*, 915–917. [CrossRef] [PubMed]
10. Russell, A.E.; Cambardella, C.A.; Laird, D.A.; Jaynes, D.B.; Meek, D.W. Nitrogen fertilizer effects on soil carbon balances in Midwestern U. S. agricultural systems. *Ecol. Appl.* **2009**, *19*, 1102–1113. [CrossRef]
11. Luo, Y. Terrestrial carbon–cycle feedback to climate warming. *Annu. Rev. Ecol. Evol. Syst.* **2007**, *38*, 683–712. [CrossRef]
12. Bardgett, R.D.; Freeman, C.; Osfle, N.J. Microbial contributions to climate change through carbon cycle feedbacks. *Int. Soc. Microb. Ecol. J.* **2008**, *2*, 805–814. [CrossRef] [PubMed]

13. Trumbore, S.E.; Chadwiek, O.A.; Amundson, R. Rapid exchanges between soil carbon and atmospheric carbon dioxide driven by temperature. *Science* **1996**, *272*, 393–396. [CrossRef]
14. Qin, Y.; Yi, S.; Ren, S.; Li, N.; Chen, J. Responses of typical grasslands in a semi–Arid basin on the Qinghai. Tibetan Plateau to climate change and disturbance. *Environ. Earth Sci.* **2014**, *71*, 1421–1431. [CrossRef]
15. Salmo, S.G.; Lovelock, C.; Duke, N.C. Vegetation and soil characteristics as indicators of restoration trajectories in restored mangroves. *Hydrobiologia* **2013**, *720*, 1–18. [CrossRef]
16. Steinbeiss, S.; Temperton, V.M.; Gleixner, G. Mechanisms of short-term soil carbon stock in experimental grasslands. *Soil Biol. Biochem.* **2008**, *40*, 2634–2642. [CrossRef]
17. Erfanzadeh, R.; Bahrami, B.; Motamedi, J.; Jullien, P. Changes in soil organic matter driven by shifts in CO-dominant plant species in a grassland. *Geoderma* **2014**, *213*, 74–78. [CrossRef]
18. Dai, W.; Huang, Y. Relation of soil organic matter concentration to climate and altitude in zonal soils of China. *Catena* **2006**, *65*, 87–94. [CrossRef]
19. Xie, X.L.; Sun, B.; Zhou, H.Z.; Lu, Z.P. Soil carbon stocks and their influencing factors under native vegetations in China. *Acta Pedol. Sin.* **2004**, *41*, 687–699.
20. Tu, J.; Xia, Z.G. Examining spatially varying relationships between land use and water quality using geographically weighted regression I: Model design and evaluation. *Sci. Total Environ.* **2008**, *407*, 358–378. [CrossRef]
21. Nishimura, S.; Yonemura, S.; Sawamoto, T.; Shirato, Y.; Akiyama, H.; Sudo, S. Effect of land use change from paddy rice cultivation to upland crop cultivation on soil carbon budget of a cropland in Japan. *Agric. Ecosyst. Environ.* **2008**, *125*, 9–20. [CrossRef]
22. Spackman, L.K.; Munn, L.C. Genesis and morphology of soils associated with formation of laramie basin (mima-like) mounds in wyoming. *Soil Sci. Soc. Am. J.* **1985**, *48*, 1384–1392. [CrossRef]
23. Ayanaba, A.; Jenkinson, D.S. Decomposition of carbon-14 labeled Ryegrass and Maize under tropical conditions. *Soil Sci. Soc. Am. J.* **1990**, *54*, 112–115. [CrossRef]
24. Costa, E.M.; Tassinari, W.D.S.; Pinheiro, H.S.K.; Beutler, S.J.; Dos Anjos, L.H.C. Mapping soil organic carbon and organic matter fractions by geographically weighted regression. *J. Environ. Qual.* **2018**, *47*, 718–725. [CrossRef]
25. Tan, X.; Guo, P.T.; Wu, W.; Li, M.F.; Liu, H.B. Prediction of soil properties by using geographically weighted regression at a regional scale. *Soil Res.* **2017**, *55*, 318–331. [CrossRef]
26. Meersmans, J.; de Ridder, F.; Canters, F.; de Baets, S.; van Molle, M. A multiple regression approach to assess the spatial distribution of soil organic carbon (SOC) at the regional scale (Flanders, Belgium). *Geoderma* **2008**, *143*, 1–13. [CrossRef]
27. Amare, T.; Hergarten, C.; Hurni, H.; Wolfgramm, B.; Yitaferu, B.; Selassie, Y.G. Prediction of soil organic carbon for Ethiopian highlands using soil spectroscopy. *ISRN Soil Sci.* **2013**, *2013*, 720589. [CrossRef]
28. Yang, Y.; Fang, J.; Tang, Y.; Ji, C.; Zheng, C.; He, J.; Zhu, B. Storage, patterns and controls of soil organic carbon in the Tibetan grasslands. *Glob. Chang. Biol.* **2008**, *14*, 1592–1599. [CrossRef]
29. Doetterl, S.; Stevens, A.; van Oost, K.; Quine, T.A.; van Wesemael, B. Spatially explicit regional scale prediction of soil organic carbon stocks in cropland using environmental variables and mixed model approaches. *Geoderma* **2013**, *204–205*, 31–42. [CrossRef]
30. Fotheringham, A.S.; Brunsdon, C.; Charlton, M.E. *Geographically Weighted Regression: The Analysis of Spatially Varying Relationships*; Wiley: Chichester, UK, 2002.
31. Scull, P. A top-down approach to the state factor paradigm for use in macroscale soil analysis. *Ann. Assoc. Am. Geogr.* **2010**, *100*, 1–12. [CrossRef]
32. Harris, P.; Fotheringham, A.; Crespo, R.; Charlton, M. The use of geographically weighted regression for spatial prediction: An evaluation of models using simulated data sets. *Math. Geosci.* **2010**, *42*, 657–680. [CrossRef]
33. McBratney, A.B.; Santos, M.M.; Minasny, B. On digital soil mapping. *Geoderma* **2003**, *117*, 3–52. [CrossRef]
34. Minasny, B.; Hartemink, A.E. Predicting soil properties in the tropics. *Earth Sci. Rev.* **2011**, *106*, 52–62. [CrossRef]
35. Taghizadeh-Mehrjardi, R.; Nabiollahi, K.; Kerry, R. Digital mapping of soil organic at multiple depths using different data mining techniques in Baneh region, Iran. *Geoderma* **2016**, *266*, 98–110. [CrossRef]
36. Forkuor, G.; Hounkpatin, O.K.; Welp, G.; Thiel, M. High resolution mapping of soil properties using remote sensing variables in South-Western Burkina Faso: A comparison of machine learning and multiple linear regression models. *PLoS ONE* **2017**, *12*, e0170478. [CrossRef] [PubMed]
37. Drake, J.M.; Randin, C.; Guisan, A. Modelling ecological niches with support vector machines. *J. Appl. Ecol.* **2006**, *43*, 424–432. [CrossRef]
38. Gautam, R.; Panigrahi, S.; Franzen, D.; Sims, A. Residual soil nitrate prediction from imagery and non-imagery information using neural network technique. *Biosyst. Eng.* **2011**, *110*, 20–28. [CrossRef]
39. Khlosi, M.; Alhamdoosh, M.; Doualk, A.; Gabriels, D.; Cornelis, W.M. Enhanced pedotransfer functions with support vector machines to predict water retention of calcareous soil. *Eur. J. Soil Sci.* **2016**, *67*, 276–284. [CrossRef]
40. Nguyen, P.M.; Haghverdi, A.; Pue, J.D.; Botula, Y.D.; Le, K.V.; Waegeman, W.; Cornelis, W.M. Comparison of statistical regression and data-mining techniques in estimating soil water retention of tropical delta soils. *Biosyst. Eng.* **2017**, *153*, 12–27. [CrossRef]
41. Krishna, G.; Sahoo, R.N.; Singh, P.; Bajpai, V.; Patra, H.; Kumar, S.; Dandapani, R.; Gupta, V.K.; Viswanathan, C.; Ahmad, T.; et al. Comparison of various modelling approaches for water deficit stress monitoring in rice crop through hyperspectral remote sensing. *Agric. Water Manag.* **2019**, *213*, 231–244. [CrossRef]
42. Gunn, S.R. *Support Vector Machines for Classification and Regression*; University of Southampton: Southampton, UK, 1998.

43. Wang, X.Q.; Zhang, B.M.; Nie, L.S.; Wang, W.; Zhou, J.; Xu, S.F.; Chi, Q.H.; Liu, D.S.; Liu, H.L.; Han, Z.X.; et al. Mapping Chemical Earth Program: Progress and challenge. *J. Geochem. Explor.* **2020**, *217*, 106578. [CrossRef]
44. Liu, H.; Zhang, Y.; Yang, J.; Wang, H.; Hu, W. Quantitative source apportionment, risk assessment and distribution of heavy metals in agricultural soils from southern Shandong Peninsula of China. *Sci Total Environ.* **2021**, *767*, 144879. [CrossRef] [PubMed]
45. Wang, X.Q.; The CGB Sampling Team. China Geochemical Baselines: Sampling methodology. *J. Geochem. Explor.* **2014**, *148*, 25–39. [CrossRef]
46. Wang, X.Q.; Han, Z.X.; Wang, W.; Zhang, B.M.; Wu, H.; Nie, L.S.; Zhou, J.J.; Chi, Q.H.; Xu, S.F.; Liu, H.L.; et al. Continental-scale geochemical survey of lead (Pb) in mainland China's pedosphere: Concentration, spatial distribution and influences. *Appl. Geochem.* **2019**, *100*, 55–63. [CrossRef]
47. Wen, Y.; Li, W.; Yang, Z.; Zhang, Q.; Ji, J. Enrichment and source identification of Cd and other heavy metals in soils with high geochemical background in the karst region, Southwestern China. *Chemosphere* **2020**, *245*, 125620. [CrossRef]
48. Zhang, Q.; Bai, J.; Wang, Y. Analytical scheme and quality monitoring system for China Geochemical Baselines. *Earth Sci. Front.* **2012**, *19*, 33–42. (In Chinese with English Abstract)
49. Hartmann, J.; Moosdorf, N. The new global lithological map database GLiM: A representation of rock properties at the Earth surface. *Geochem. Geophy. Geosyst.* **2013**, *13*, Q12004. [CrossRef]
50. Breiman, L. Bagging predictors. *Mach. Learn.* **1996**, *24*, 123–140. [CrossRef]
51. Tian, M.; Wang, X.; Nie, L.; Liu, H.L.; Wang, W.; Yan, T.T. Spatial distributions and the identification of ore-related anomalies of Cu across the boundary area of China and Mongolia. *J. Geochem. Explor.* **2019**, *197*, 37–47. [CrossRef]
52. R Development Core Team. R: A Language and Environmental for Statistical Computing. 2007. Available online: http://www.R-project.org (accessed on 3 March 2023).
53. Isaaks, E.H.; Srivastava, R. *An Introduction to Applied Geostatistics*; Oxford University Press: New York, NY, USA, 1989.
54. Liu, M.Q.; Hu, F.; Chen, X.Y. A review on mechanisms of soil organic carbon stabilization. *Acta Ecol. Sin.* **2007**, *27*, 2642–2650.
55. Poirier, N.; Derenne, S.; Balesdent, J.; Mariotti, A.; Largeau, C. Isolation and analysis of the non-hydrolysable fraction of a forest soil and an arable soil (Lacadee, southwest France). *Eur. J. Soil Sci.* **2003**, *54*, 243–255. [CrossRef]
56. Xu, J.H.; Sun, Y.; Gao, L. A review of the factors influencing soil organic carbon stability. *Chin. J. Eco-Agric.* **2018**, *26*, 222–230. (In Chinese with English Abstract)
57. Wang, L.; Ying, R.R.; Shi, J.Q.; Long, T.; Lin, Y.S. Advancement in Study on Adsorption of Organic Matter on Soil Minerals and Its Mechanism. *Acta Pedol. Sin.* **2017**, *54*, 805–818. (In Chinese with English Abstract)
58. Six, J.; Bossuyt, H.; Degryze, S.; Denef, K. A history of research on the link between (micro) aggregates, soil biota, and soil organic matter dynamics. *Soil Till. Res.* **2004**, *79*, 7–31. [CrossRef]
59. Smith, A.P.; Marin-Spiotta, E.; de Graaff, M.A. Microbial community structure varies across soil organic matter aggregate pools during tropical land cover change. *Soil Biol. Biochem.* **2014**, *77*, 292–303. [CrossRef]
60. Lalonde, K.; Mucci, A.; Ouellet, A.; Gélinas, Y. Preservation of organic matter in sediments promoted by iron. *Nature* **2012**, *483*, 198–200. [CrossRef]
61. Salvadó, J.A.; Tesi, T.; Andersson, A.; Ingri, J.; Dudarev, O.V.; Semiletov, I.P.; Gustafsson, Ö. Organic Carbon Remobilized from Thawing Permafrost Is Resequestered by Reactive Iron on the Eurasian Arctic Shelf. *Geophys. Res. Lett.* **2015**, *42*, 8122–8130. [CrossRef]
62. Zhao, Q.; Poulson, S.R.; Obrist, D.; Sumaila, S.; Dynes, J.J.; McBeth, J.M.; Yang, Y. Iron-Bound Organic Carbon in Forest Soils: Quantification Andcharacterization. *Biogeosciences* **2016**, *13*, 4777–4788. [CrossRef]
63. Basile-Doelsch, I.; Amundson, R.; Stone, W.E.E.; Borschneck, D.; Bottero, J.Y.; Moustier, S.; Masin, F.; Colin, F. Mineral Control of Carbon Pools in a Volcanic Soil Horizon. *Geoderma* **2007**, *137*, 477–489. [CrossRef]
64. Wiseman, C.L.S.; Püttmann, W. Interactions between Mineral Phases in the Preservation of Soil Organic Matter. *Geoderma* **2006**, *134*, 109–118. [CrossRef]
65. Huang, W.; Hammel, K.E.; Hao, J.; Thompson, A.; Timokhin, V.I.; Hall, S.J. Enrichment of Lignin-Derived Carbon in Mineral-Associated Soil Organic Matter. *Environ. Sci. Technol.* **2019**, *53*, 7522–7531. [CrossRef] [PubMed]
66. Reichstein, M.; Bahn, M.; Ciais, P.; Frank, D.; Mahecha, M.D.; Seneviratne, S.I.; Zscheischler, J.; Beer, C.; Buchmann, N.; Frank, D.C.; et al. Climate Extremes and the Carbon Cycle. *Nature* **2013**, *500*, 287–295. [CrossRef]
67. Schmidt, M.W.I.; Torn, M.S.; Abiven, S.; Dittmar, T.; Guggenberger, G.; Janssens, I.A.; Kleber, M.; Kögel-Knabner, I.; Lehmann, J.; Manning, D.A.C.; et al. Persistence of Soil Organic Matter as an Ecosystem Property. *Nature* **2011**, *478*, 49–56. [CrossRef]
68. Han, L.; Sun, K.; Jin, J.; Xing, B. Some Concepts of Soil Organic Carbon Characteristics and Mineral Interaction from a Review of Literature. *Soil Biol. Biochem.* **2016**, *94*, 107–121. [CrossRef]
69. Chen, C.; Dynes, J.J.; Wang, J.; Sparks, D.L. Properties of Fe-Organic Matter Associations via Coprecipitation versus Adsorption. *Environ. Sci. Technol.* **2014**, *48*, 13751–13759. [CrossRef] [PubMed]
70. Luo, W.; Zhang, H.H.; Chen, J.J.; Liu, Y.; Li, D.Q. Storage and spatial distributions of soil organic carbon in Guangdong Province, China. *Ecol. Environ. Sci.* **2018**, *27*, 1593–1601. (In Chinese with English Abstract)
71. Kunkel, M.L.; Flores, A.N.; Smith, T.J.; McNamara, J.P.; Benner, S.G. A Simplified Approach for Estimating Soil Carbon and Nitrogen Stocks in Semi-Arid Complex Terrain. *Geoderma* **2011**, *165*, 1–11. [CrossRef]
72. Deng, Y.J.; Wang, J.C.; Xu, J.; Wu, Y.Q.; Chen, J.Y. Spatiotemporal variation of vegetation carbon sequestration and its meteorological contribution in Guangdong Province. *Ecol. Environ. Sci.* **2022**, *31*, 1–8. (In Chinese with English Abstract)

73. Davidson, E.C.A.; Belk, E.; Boone, R.D. Soil Water Content and Temperature as Independent or Confounded Factors Controlling Soil Respiration in a Temperate Mixed Hardwood Forest. *Glob. Chang. Biol.* **1998**, *4*, 217–227. [CrossRef]
74. Fang, C.; Moncrieff, J.B. The Dependence of Soil CO_2 Efflux on Temperature. *Soil Biol.* **2001**, *33*, 155–165. [CrossRef]
75. Bao, F.; Zhou, G.S. Review of research advances in soil respiration of grassland in China. *Chin. J. Plant Ecol.* **2010**, *34*, 713–726. (In Chinese with English Abstract)